

# A Novel Sensor Based on Ag Nanoparticles Functionalized with Poly-Acid Chrome Blue K and Graphene for the Sensitive Determination of Diclofenac Sodium

Qing Huang<sup>1</sup>, Xiaokun Li<sup>1,\*</sup>, Suxiang Feng<sup>1</sup>, Wenfeng Zhuge<sup>1</sup>, Jinyun Peng<sup>2</sup>, Xiaoting Li<sup>2</sup>

<sup>1</sup> School of Pharmacy, Henan University of Traditional Chinese Medicine, Zhengzhou 450046, China

<sup>2</sup> College of Chemistry and Chemical Engineering, Guangxi Normal University for Nationalities, Chongzuo 532200, China

\*E-mail: [li96052122@126.com](mailto:li96052122@126.com)

Received: 10 May 2018 / Accepted: 20 June 2018 / Published: 5 January 2019

---

Ag nanoparticles functionalized with poly-acid chrome blue K and graphene (Ag-poly-ACBK@Gr) were successfully fabricated on the surface of a glassy carbon electrode using layer-by-layer electropolymerization. The surface structure of the synthesized modified glassy carbon electrode was characterized by scanning electron microscopy. The electrochemical behaviours of diclofenac sodium (DS) at the Ag-poly-ACBK@Gr-modified electrode were investigated by cyclic voltammetry and differential pulse voltammetry. It was found that the prepared sensor exhibited a cathodic peak at 0.78 V with higher peak current response compared to the related modified electrodes. Under optimal conditions, the sensor for the determination of DS exhibits a good linear relationship between the peak current and DS concentration in the range from 0.1 to 40  $\mu\text{M}$ , and the equation is  $I_p(\mu\text{A}) = 7.23 \times 10^3 c(\mu\text{M}) + 3.46 \times 10^{-2}$  ( $R = 0.9955$ ) with the estimated limit of detection of 34.2 nM ( $S/N = 3$ ). The Ag-poly-ACBK@Gr-modified glassy carbon electrode with high sensitivity and excellent stability and selectivity was successfully applied to detect DS in real drugs and human urine at the recoveries ranging from 99.60 to 101.84%.

---

**Keywords:** Ag-poly-ACBK@Gr; Diclofenac sodium; Electrochemistry

## 1. INTRODUCTION

Diclofenac sodium (DS) is well-known as a non-steroidal anti-inflammatory drug that has been used to treat a variety of inflammatory diseases including scapulohumeral periarthritis, osteoarthritis and degenerative joints [1-2]. However, DS may cause some side effects such as haemodynamic changes or thyroid tumours [3-4]. It has a potential hazardous compound in natural water bodies, generating some pollution [5]. Currently, DS contamination has been slowed down owing to the use of the adsorption technique [2, 6]. However, it is still necessary to develop a method for trace detection of

DS in pharmaceutical preparations. In recent years, common techniques such as the UV spectrophotometric method [7], high-performance liquid chromatography [8], fluorometry [9] and electrochemistry [10] have been applied to the quality monitoring of DS. It is worth noting that electrochemistry was applied to trace detection with some advantages of high sensitivity, low limit of detection, fast testing speed and simple equipment and low cost [11-14]. The current study presents a novel sensor based on a strategy to achieve ultra-sensitive DS determination.

Chemically modified electrodes refer to the molecular design on the surface of the electrode. This approach fixes the molecules, ions or polymers with excellent chemical properties on the surface of the electrodes in the form of a chemical film, conferring some specific chemical and electrochemical properties on the electrodes [15-16]. Electroactive polymer-modified electrodes have attracted wide attention due to their high sensitivity and excellent adsorption capacity [17]. In addition, electrical polymerization techniques not only are simple and easy to carry out but also can be used for the control of the film thickness [18]. Therefore, this approach has been widely used in biology, environment analysis, chemical analysis, medicine and other fields [15].

Acidic chrome blue K (ACBK), a kind of dyestuff with electrochemical catalytic activity, usually plays the role of the redox indicator in chemistry titration [19]. Meanwhile, it is also an organic conjugate compound with special structure [20]. ACBK was fixed on the electrode surface using electropolymerization, and then, a polymer film, such as poly(methylene blue) [21], polyazulene [22], and poly(glycine) [23], was obtained. Graphene (Gr) is a thin carbon material with excellent conductivity and mechanical properties [24]. It is now used in biology, medicine and electricity analysis owing to its large specific surface area and biocompatibility [25-26]. Therefore, the composite of ACBK and Gr is used as an electrochemical polymerization modified glassy carbon electrode (poly-ACBK@Gr/GCE) to obtain larger active surface, better conductivity, and higher stability [27]. Ag nanoparticles have high medical value owing to their good fungal resistance [28-29]. Moreover, Ag nanoparticles are extremely popular with researchers because of their advantages of large surface areas, special binding sites, nontoxicity, and strong conductivity [30].

In the work, based on the poly-ACBK@Gr/GCE platform, Ag nanoparticles were uniformly fixed on the surface of poly-ACBK@Gr using a layer-by-layer of electropolymerization to obtain the composite film, namely, Ag nanoparticles functionalized with poly-ACBK@Gr (Ag-poly-ACBK@Gr). The thickness of the composite film could be controlled, and the overall electro-catalytic performance was improved. The Ag-poly-ACBK@Gr-modified GCE was applied for the determination of DS by differential pulse voltammetry (DPV) with excellent response. There are no previous reports on the direct electrochemical measurement of DS based on Ag-poly-ACBK@Gr. Therefore, this strategy should be considered.

## 2. EXPERIMENTAL SECTION

### 2.1. Reagents and instruments

Diclofenac sodium sustained-release tablets and capsules were obtained from Xinyi Pharmaceutical Co., LTD (China, Shanghai) and Simcere Pharmaceutical group (China, Hainan),

respectively. ACBK was purchased from the Guangzhou chemical reagent factory in China. Other reagents were obtained from Aladdin industrial corporation (Shanghai, China) and were of analytical grade. Phosphate buffer solution (PBS) was used as the electrolyte and was prepared using 0.2 M  $\text{Na}_2\text{HPO}_4$  and 0.2 M  $\text{KH}_2\text{PO}_4$  solution containing 0.1 M NaCl.

The surface morphologies of poly-ACBK@Gr and Ag-poly-ACBK@Gr were examined by scanning electron microscopy (SEM, ZEISS EVO18, Germany). The electrochemical experiments were performed using a CHI660D electrochemical workstation (ChenHua Instruments Co., Shanghai, China) with a three-electrode system: a GCE with the diameter of 3 mm was used as the working electrode, a calcium electrode was used as the indicator electrode, and a calomel electrode was used as the reference electrode.

## 2.2. Fabrication of Ag-poly-ACBK@Gr/GCE

Graphene oxide (GO) was obtained by the Hummers method [31]. One hundred milligrams of synthesized GO was dispersed into 50 mL deionized water by ultrasonication to obtain a suspension which was reduced in 80 °C for 2 h after the addition of 1 g of  $\text{NaBH}_4$ . The product was cleaned with deionized water, and Gr was obtained via vacuum drying at 45 °C for 12 h [32]; 0.5 mg of obtained Gr was dispersed in 1 mL of 1 mM ACBK solution to prepare the ACBK@Gr suspension. The glassy carbon electrode (GCE) was polished to a mirror-like finish with 1.0, 0.3 and 0.05  $\mu\text{m}$  alumina polishing solutions, respectively, and then rinsed with deionized water and dried by high-purity nitrogen. The procedure for the fabrication Ag-poly-ACBK@Gr-modified GCE was as follows: in the first step, the bare GCE was immersed into the ACBK@Gr suspension and the potential range from -1.4 V to 0.2 V was swept in 40 segments at the scan rate 50  $\text{mV s}^{-1}$ , and a poly-ACBK@Gr film on the surface of GCE was obtained. Second, the poly-ACBK@Gr modified GCE continued to be immersed into 1 mM  $\text{AgNO}_3$  containing 0.1 M  $\text{KNO}_3$  solution, and the potential range from -1.5 V to 2.1 V was swept for 20 segments at the scan rate 100  $\text{mV s}^{-1}$ , and Ag functionalized with poly-ACBK@Gr modified GCE was prepared successfully, and then the Ag-poly-ACBK@Gr/GCE was rinsed with deionized water for further expansion. For comparison, Gr/GCE, ACBK@GCE and poly-ACBK@Gr/GCE were fabricated using similar procedures.

## 2.3. Procedure for real samples

Five diclofenac sodium sustained release tablets were ground into powder and weighed accurately to obtain the DS amount of one sample. The sample amount was dissolved into 50 mL of PBS (0.2 M) solution using ultrasonication and transferred into a 250 mL volumetric flask after filtration, followed by dilution with PBS solution to volume. The preparation of the sample was thus completed. The diclofenac sodium sustained release capsules sample was prepared using a similar method.

### 3. RESULTS AND DISCUSSION

#### 3.1. Characterization of modified GCE

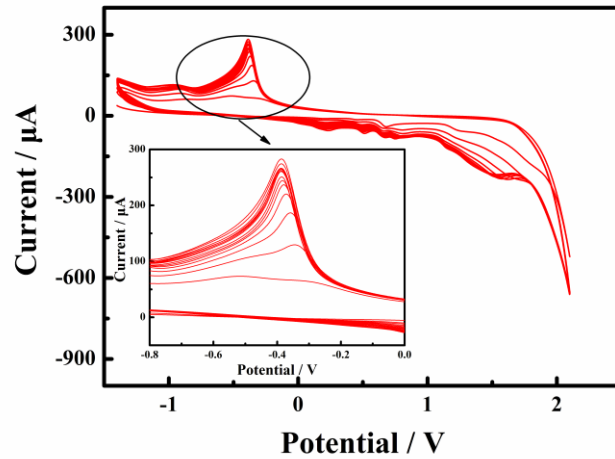


**Figure 1.** CVs of functionalization of Ag nanoparticles on the surface of poly-ACBK@Gr/GCE in 1 mM AgNO<sub>3</sub> containing 0.1 M KNO<sub>3</sub> solution. The cycling number is 28. Inset: enlarged image.

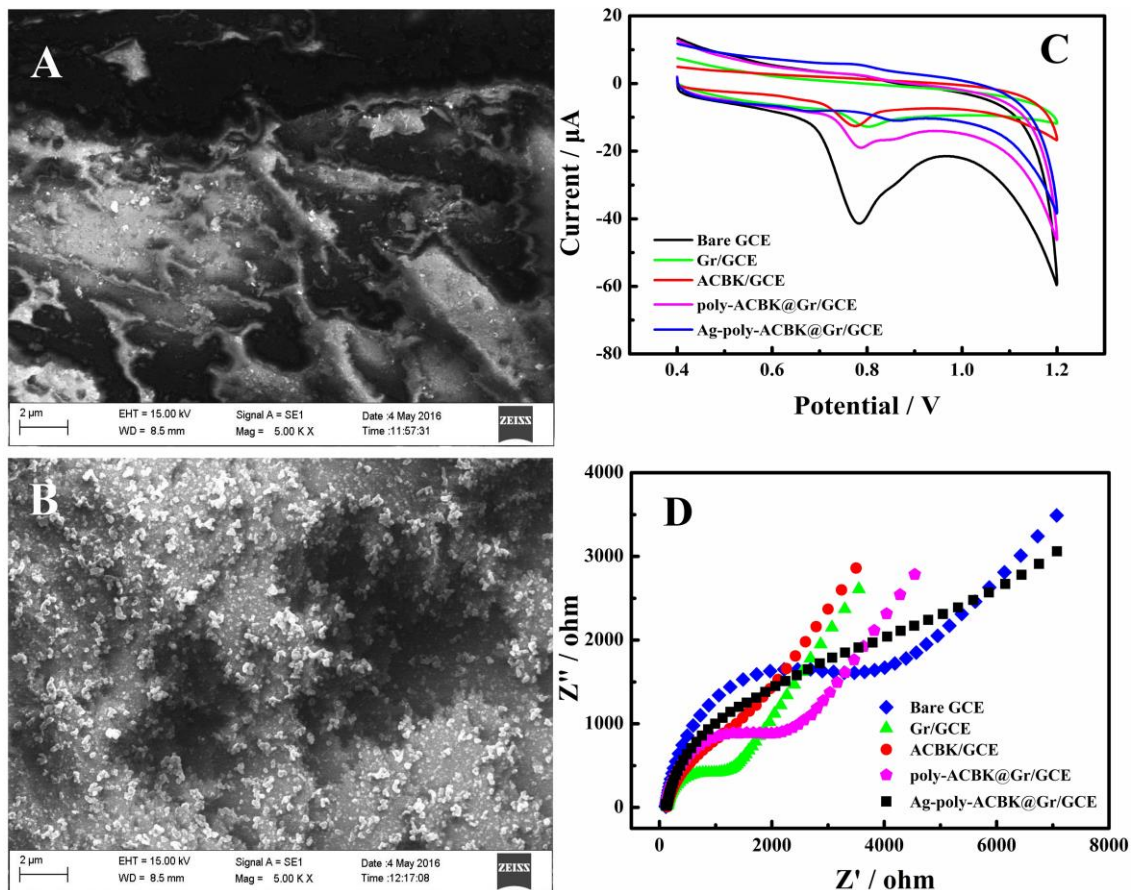


**Figure 2.** SEM images of the surface of (A) poly-ACBK@Gr/GCE and (B) Ag-poly-ACBK@Gr/GCE. The (C) CVs and (D) EIS of bare GCE, Gr/GCE, ACBK/GCE, poly-ACBK@Gr/GCE, Ag-poly-ACBK@Gr/GCE.

The poly-ACBK@Gr/GCE was swept continuously at the potential range from -1.5 V to 2.1 V for 28 cycles at the scan rate  $100 \text{ mV s}^{-1}$  in  $1 \text{ mM AgNO}_3$  containing  $0.1 \text{ M KNO}_3$  to obtain a film of Ag-poly-ACBK@Gr on the surface of GCE. The cyclic voltammetry curves (CVs) are shown in Fig. 1, and an anodic peak current at about  $-0.35 \text{ V}$  increasing with the cycling number is observed and tends to be stable after 16 segments. It was indicated that Ag nanoparticles were modified successfully on the surface of poly-ACBK@Gr/GCE.

The surface morphologies of poly-ACBK@Gr/GCE and Ag-poly-ACBK@Gr/GCE were characterized by SEM (Figs. 2A and B). A thin film with pleated construction on the GCE can be clearly seen in Fig. 2A, indicating that Gr can become a modified GCE through electro-deposition [21]. Furthermore, the composite of ACBK and Gr shows enhanced surface area to provide more opportunity for further functionalization. An examination of Fig. 2B shows that many Ag nanoparticles were immobilized on the rough surface of poly-ACBK@Gr/GCE, and the sizes of the Ag nanoparticles are in the range from 20 to 30 nm. The morphology is in agreement with the results of the previous work [21]. The addition of Ag nanoparticles enables the whole material to obtain a larger surface area which directly contributes to the enhancement of adsorption behaviour.

The cyclic voltammetry curves (CVs) for bare GCE, Gr/GCE, ACBK/GCE, poly-ACBK@Gr/GCE, Ag-poly-ACBK@Gr/GCE in  $0.2 \text{ M PBS}$  ( $\text{pH } 2.5$ ) buffer containing  $20 \text{ }\mu\text{M DS}$  at the scan rate of  $0.1 \text{ V s}^{-1}$  are shown in Fig. 2C. A cathodic peak potential ( $E_p$ ) on Ag-poly-ACBK@Gr/GCE was found at  $0.78 \text{ V}$ , and the corresponding peak current ( $I$ ,  $29.01 \text{ }\mu\text{A}$ ), by contrast, was 17 times that of bare GCE ( $1.68 \text{ }\mu\text{A}$ ). It was demonstrated that the catalytic efficacy to DS at Ag-poly-ACBK@Gr/GCE was substantially improved, and the method was expected to be applicable for further quantitative determination. Electrochemical impedance spectroscopy (EIS) of different modified electrodes was carried out in  $5 \text{ mM } [\text{Fe}(\text{CN})_6]^{3-/4-}$  solution containing  $0.1 \text{ M KCl}$  with the same parameters. As displayed in Fig. 2D, in the low-frequency region, the diameters of Gr/GCE and ACBK/GCE were smaller than those for the bare GCEs, indicating that Gr and ACBK showed a low charge transfer resistance. However, the diameter of Ag-poly-ACBK@Gr/GCE is greater than that of the poly-ACBK@Gr/GCEs. According to Fuchs' theory [33], the phenomenon of decrease in the conductivity is attributed to the additional scattering at the surface of poly-ACBK@Gr/GCE when the electron mean free path becomes comparable to the thickness of the metal film. The results demonstrated that silver ions in silver nitrate had been transformed into Ag nanomaterials through electrochemical deposition, and the Ag nanomaterials had successfully modified the film of poly-ACBK@Gr.

### 3.2. Effect of pH

The electrochemical responses of DS at the Ag-poly-ACBK@Gr/GCE in different pH PBS buffer are shown in Fig. 3. The cathodic peak current was decreasing with increasing pH values in the range from 2.5 to 7.0 and decreased rapidly in PBS solution at a pH of 2. Hence, PBS buffer at a pH of 2.5 was used in the subsequent steps. Furthermore, the cathodic peak potential decreased with increasing pH values from 2.0 to 7.0 and showed a good linear relationship with the pH. The equation

of linear regression is  $E_p(\text{V}) = -0.035\text{pH} + 0.90$ ,  $R=0.9960$ . According to the theoretical equation [34]  $E_p = -0.059(m/n)\text{pH} + E^\theta$ , it is demonstrated that the numbers of proton transferred ( $m$ ) were not equal to electron transferred ( $n$ ) in the electrochemical reaction of DS, and the ratio ( $m/n$ ) was calculated to be 0.59. The results may be ascribed to the formation of the ACBK@Gr polymer corresponding to unequal proton/electron reaction on the nanoparticles film [35]. The variation of the ratio was also discussed in nanohybrid film/microperoxidase [36].

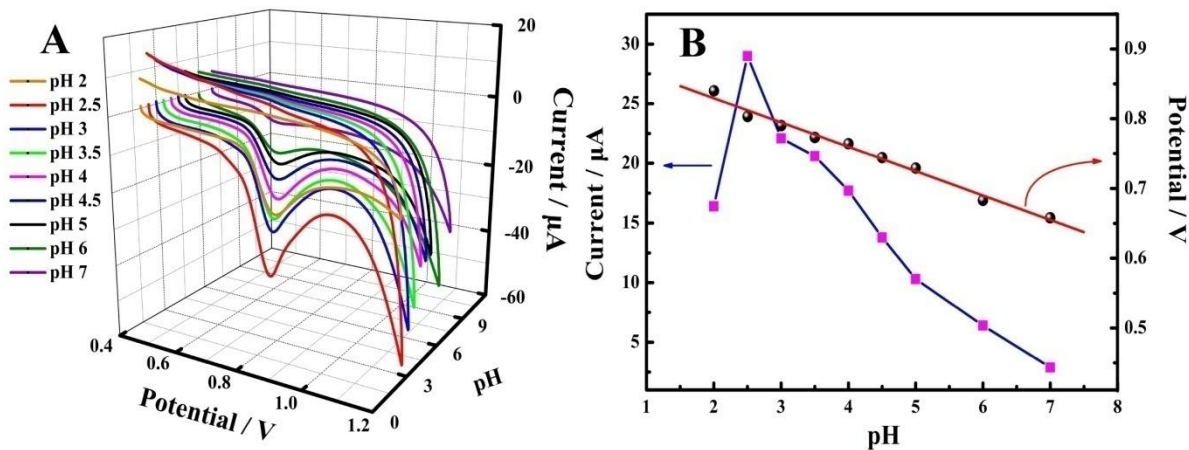


**Figure 3.** Influence of (A) pH in PBS solution containing 20  $\mu\text{M}$  DS. (B) Corresponding data.

### 3.3. Effect of scan rates

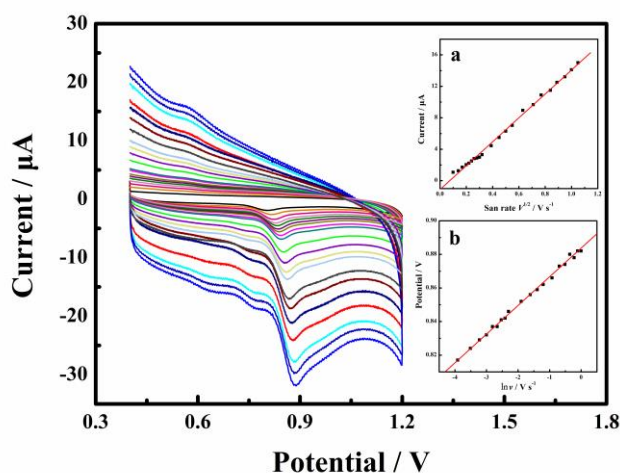
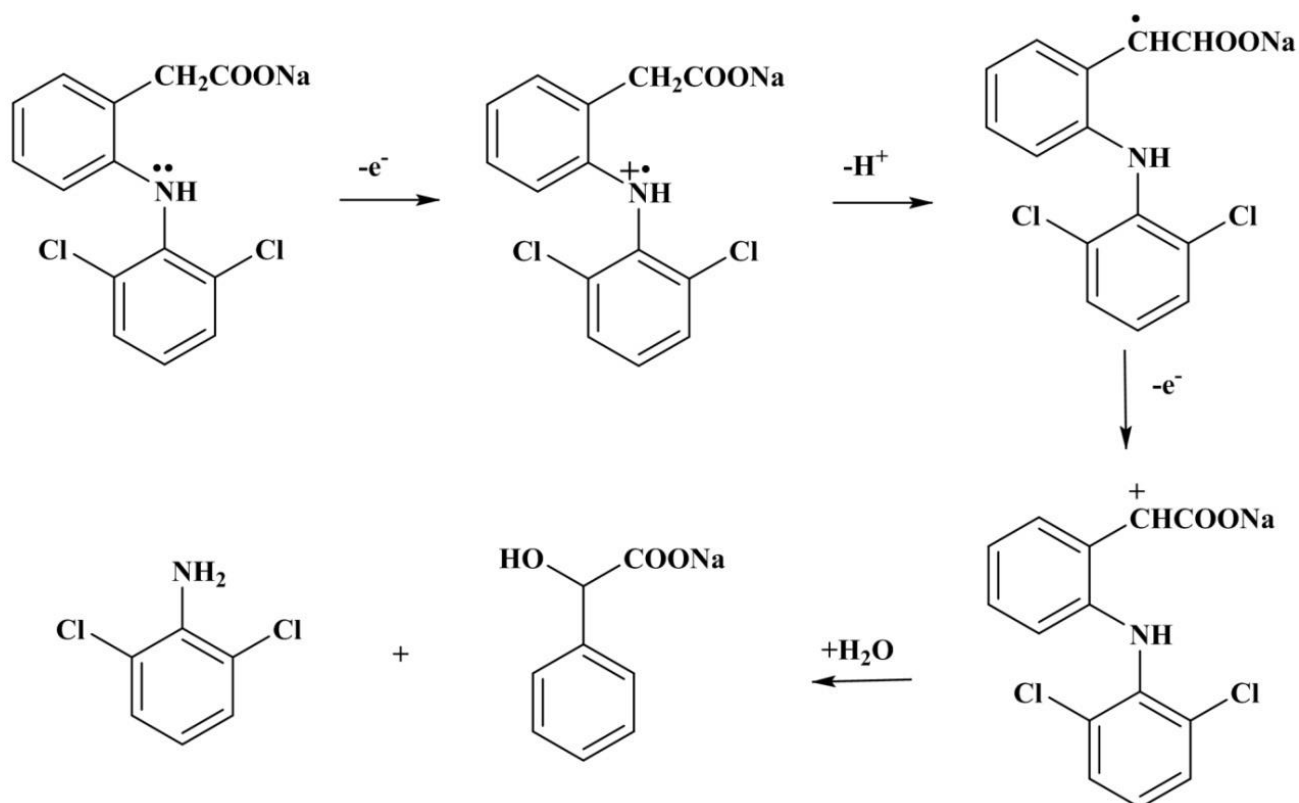


**Figure 4.** CVs of DS in pH 2.5 PBS buffer at different scan rates in the range from 0.01 to 0.12  $\text{V s}^{-1}$ . Inset a: linear relationship of peak current ( $I_p$ ) and the square root of scan rate ( $v^{1/2}$ ). Inset b: the linear relationship of peak potential ( $E_p$ ) and logarithm of scan rates ( $\ln v$ ).

Fig. 4 shows the CVs of the Ag-poly-ACBK@Gr/GCE in PBS buffer containing 10  $\mu\text{M}$  DS scan rates in the range from 0.01 to 0.12  $\text{V s}^{-1}$ . The cathodic peak current ( $I_p$ ) reveals a good linear relationship with the square root of the scan rate ( $v^{1/2}$ ), and the equation is  $I_p(\mu\text{A}) = -15.20v^{1/2} + 1.12$ ,  $R = 0.9983$ . This outcome indicated that the electrocatalysis for DS at the Ag-poly-ACBK@Gr/GCE

was essentially controlled by diffusion. The peak potential shows a positive drift with linearity and the equation is  $E_p = 0.0176 \ln v + 0.8843$ ,  $R = 0.9968$ . The irreversible reduction in DS with the scan rate increases by 10 times, and  $E_p$  shifts positively by  $1.15 RT/\alpha F$  units [ $R$  is the gas constant,  $8.314 \text{ J} (\text{mol} \cdot \text{K})^{-1}$ ;  $T$  is thermodynamic temperature,  $298.15 \text{ K}$ ;  $F$  is the Faraday constant,  $96,485 \text{ C mol}^{-1}$ ;  $\alpha$  is the electron transfer coefficient]. According to Laviron's equation [37],  $\alpha$  and  $n$  were calculated to be 0.62 and 2.30 (approximately equal to 2), respectively. The results showed that the electrochemical behaviours of DS are reduction reactions with two-electron transfer and one-proton transfer. The mechanism of the reaction on the Ag-poly-ACBK@Gr/GCE is presented in Scheme 1.



**Scheme 1.** Electrochemical mechanism of DS detection at the Ag-poly-ACBK@Gr/GCE.

#### 3.4. Chronocoulometry studies

The effective surface area was investigated for different modified electrodes in  $1 \text{ mM}$   $[\text{Fe}(\text{CN})_6]^{3-/4-}$  solution containing  $0.1 \text{ M}$   $\text{KCl}$  by the chronocoulometry (CC) technique. As shown in Fig. 5, bare GCE, Gr/GCE, ACBK/GCE, poly-ACBK@Gr/GCE and Ag-poly-ACBK@Gr/GCE show five different curves and present five different relationships between the change ( $Q$ ) and potential pulse width ( $t^{1/2}$ ). The linear equations are given by  $Q(\mu\text{A}) = 13.89t^{1/2} + 29.82$  ( $R=0.9970$ ),  $Q(\mu\text{A}) = 15.55t^{1/2} + 41.42$  ( $R = 0.9978$ ),  $Q(\mu\text{A}) = 16.91t^{1/2} + 38.89$  ( $R=0.9964$ ),  $Q(\mu\text{A}) = 25.54t^{1/2} + 20.87$  ( $R = 0.9999$ ) and  $Q(\mu\text{A}) = 53.04t^{1/2} + 57.52$  ( $R = 0.9989$ ), respectively. According to Anson's equation [38], the effective surface area values of the modified electrodes were calculated as  $0.13 \text{ cm}^2$ ,  $0.14 \text{ cm}^2$ ,  $0.16 \text{ cm}^2$ ,  $0.24 \text{ cm}^2$  and  $0.50 \text{ cm}^2$ , respectively. This outcome showed that the effective working area has

been improved after GEC was fabricated by layer-by-layer electropolymerization. Specifically, the addition of Ag nanoparticles enabled a great improvement in the effective surface area of the electrode.

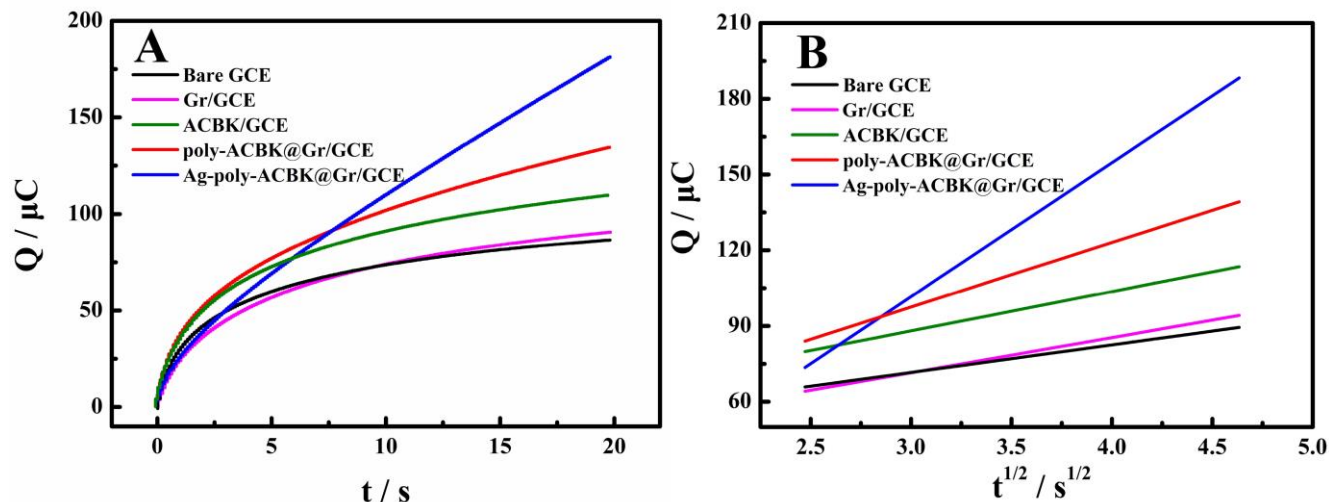


**Figure 5.** Plot of (A)  $Q \sim t$  and  $Q \sim t^{1/2}$  curve of bare/GCE, Gr/GCE, ACBK/GCE, poly-ACBK@Gr/GCE, Ag-poly-ACBK@Gr/GCE.

### 3.5. DS determination

Fig. 6 shows the differential pulse voltammetry curves (DPVs) of Ag-poly-ACBK@Gr/GCE for a series of DS concentrations under optimal conditions. As seen, the cathodic peak current increases with DS concentration increasing and presents a good linear relationship at the DS concentration range from 0.1 to 40  $\mu\text{M}$ .

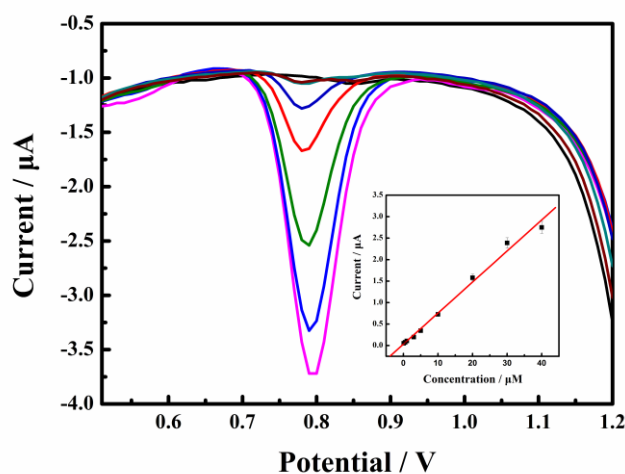


**Figure 6.** DPVs of Ag-poly-ACBK@Gr/GCE in different DS concentrations in the range from 0.1 to 40  $\mu\text{M}$ .

The equation can be expressed as  $I_p(\mu\text{A}) = 7.23 \times 10^3 c (\mu\text{M}) + 3.46 \times 10^{-2}$  ( $R = 0.9955$ ). Meanwhile, the limit of detection (LOD) is 34.2 nM. Due to the electroactive polymer with a large

active surface area and excellent electrocatalytic activity of Ag-poly-ACBK@Gr, DS concentration in the surface layer of Ag-poly-ACBK@Gr/GCE effectively increases its peak current. The comparison of Ag-poly-ACBK@Gr/GCE with other recent studies for DS detection is presented in Table. 1. The initial concentration of the linear range of the prepared sensor was lower than those for other electrochemical sensors, and the limit of detection was superior to most sensors. These results indicated that the Ag-poly-ACBK@Gr can be applied for the monitoring of DS with excellent linear concentration range, considerable sensitivity and a low limit of detection.

**Table 1.** Comparison of Ag-poly-ACBK@Gr/GCE to other recent DS detection studies.

Materials/Methods	Linear range ( $\mu\text{M}$ )	LOD (nM)	r	References
Cu-ZEGE <sup>a</sup> /DPV	0.3 ~ 20	50	0.9980	39
MWCNTs-CTS-Cu <sup>b</sup> /SWV <sup>c</sup>	0.3 ~ 200	21	0.9995	40
DBA <sup>d</sup> /DPV	0 ~ 1000	270	0.9990	41
MWCNTs- PGE <sup>e</sup> /DPV	0.047 ~ 12.95	17	0.9999	42
VFMCNTPE <sup>f</sup> /SWV	0.2 ~ 600	90	0.9980	43
TCPE <sup>g</sup> /DPV	10 ~ 140	3280	0.9952	44
MWCNTs-Cu(OH) <sub>2</sub> /DPV	0.18 ~ 119	40	0.9940	45
IL-CNTPE <sup>h</sup> /DPV	0.5 ~ 300	200	0.9950	46
GO-COOH/LSV <sup>i</sup>	1.2 ~ 400	90	0.9975	47
MWCNTs-surfactant/LSV	0.17 ~ 2.5	80	0.9920	48
Carbon nanotube paste/NPV <sup>j</sup>	2 ~ 100	800	-	49
Ag-poly-ACBK@Gr/DPV	0.1 ~ 40	34.2	0.9955	This work

<sup>a</sup> Cu-doped zeolite-modified expanded graphite-epoxy composite. <sup>b</sup> Copper ions on MWCNTS-Chitosan thin film. <sup>c</sup> Square wave voltammetry. <sup>d</sup> Amino-functionalized diclofenac binding aptamer. <sup>e</sup> Multiwalled carbon nanotubes modified pencil graphite electrode. <sup>f</sup> Vinylferrocene modified multiwall carbon nanotubes paste electrode <sup>g</sup> Tyrosine-modified carbon paste electrode <sup>h</sup> Ionic liquid-modified carbon nanotubes paste electrode. <sup>i</sup> Linear sweep voltammetric. <sup>j</sup> Normal pulse voltammetry.

### 3.5. Reproducibility, stability and selectivity

Five electrodes were modified in the same manner for the detection of 20  $\mu\text{M}$  DS under the same conditions, and the obtained peak currents were 1.70  $\mu\text{A}$ , 1.66  $\mu\text{A}$ , 1.63  $\mu\text{A}$ , 1.67  $\mu\text{A}$  and 1.64  $\mu\text{A}$ . The calculated relative standard deviation (RSD) of the Ag-poly-ACBK@Gr/GCE was 1.65%, indicating that the sensor had an excellent reproducibility. Furthermore, the stability of the sensor was investigated. The Ag-poly-ACBK@Gr/GCE was stored in a refrigerator at 4 °C for 7 days; 95.33% of its initial peak current was obtained for DS detection, indicating that the sensor shows strong stability.

To study the selectivity of the prepared sensor, several common ions were investigated, including Na<sup>+</sup>, K<sup>+</sup>, Fe<sup>3+</sup>, Mg<sup>2+</sup>, Al<sup>3+</sup>, Zn<sup>2+</sup>, Cu<sup>2+</sup>, Ca<sup>2+</sup>, NH<sup>4+</sup>, and NO<sup>2-</sup>, and these ions did not show interference effects. Furthermore, some common substances in drug formulations and the human body,

including glucose, lactose, sucrose, soluble starch, dextrin, uric acid and urea, did not interfere with the detection of DS. The 1  $\mu\text{M}$  DS solution contained 100  $\mu\text{M}$  interference. This outcome demonstrated that the designed sensor has an excellent selectivity.

### 3.6. Real samples analysis

**Table 2.** Results of DS detection for sustained release tablets, capsules and human urine samples.

Sample	Initial DS in the sample ( $\mu\text{M}$ )	Added DS concentration ( $\mu\text{M}$ )	The detection concentration ( $\mu\text{M}$ )	Recovery $\pm$ RSD (% , n=5)
Tablets	22.4	6.07	28.5	101.13 $\pm$ 1.12
Capsules	24.6	3.06	27.7	101.84 $\pm$ 1.81
Urine	0	10.00	9.96	99.60 $\pm$ 0.40

To verify the feasibility of the use of Ag-poly-ACBK@Gr/GCE for DS detection in real samples, diclofenac sodium-sustained release tablets, capsules and human urine were studied by using the standard addition method. The results are shown in Table. 2, and it can be seen that RSD was no greater than 2% and that the standard recovery rate was in the range from 99.60 to 101.84%. It was demonstrated that the Ag-poly-ACBK@Gr/GCE could be applied for the determination of human urine and different doses of real DS samples.

## 4. CONCLUSION

In this work, we have prepared a novel sensor based on Ag-poly-ACBK@Gr electro-chemical material-modified glassy carbon electrodes by using layer-by-layer electropolymerization, with larger working surface area and special structures. The prepared sensor shows excellent electrocatalytic efficiency towards DS, with the advantages of high sensitivity, stability and selectivity. Meanwhile, it exhibits a low detection limit of 34.2 nM and linear range from 0.1 to 40  $\mu\text{M}$  for DS. Furthermore, it could be applied to the detection of DS in human urine and related drugs.

## ACKNOWLEDGEMENTS

The authors wish to thank the National Natural Science Foundation of China (Grant No. 21465004) for fellowships and financial support.

## References

1. M. Shalauddin, S. Akhter, S. Bagheri, M.S. Abd Karim, N. Adib Kadri, W.J. Basirun, *Int. J. Hydrogen Energy*, 42(31) (2017) 19951-19960.
2. Z. Hasan, N.A. Khan, S.H. Jung, *Chem. Eng. J.*, 284 (2016) 1406-1413.

3. Q. Huang, S. Deng, D. Shan, Y. Wang, B. Wang, J. Huang, G. Yu, *J. Colloid Interface Sci.*, 488 (2017) 142-148.
4. A. Afkhami, A. Bahiraei, T. Madrakian, *Mater Sci Eng C Mater Biol Appl*, 59 (2016) 168-176.
5. M. Schriks, M.B. Heringa, M.M. van der Kooi, P. de Voogt, A.P. van Wezel, *Water Res.*, 44(2) (2010) 461-76.
6. B.N. Bhadra, P.W. Seo, S.H. Jung, *Chem. Eng. J.*, 301 (2016) 27-34.
7. S. Savale, H. Mahajan, *Asian Journal of Biomaterial Research*, 3(2) (2017) 40-43
8. S.D. Labhade, S.R Chaudhari, R.B. Saudagar, *IJSRST*, 2(4) (2018) 1413-1417
9. A.A. Gouda, M.I. Kotb El-Sayed, A.S. Amin, R. El Sheikh, *Arabian J. Chem.*, 6(2) (2013) 145-163.
10. L. Kashefi-Kheyraadi, M.A. Mehrgardi, *Biosens. Bioelectron.*, 33(1) (2012) 184-9.
11. S. Gandhi, A. Talan, A. Mishra, S.A. Eremin, J. Narang, A. Kumar, *Biosens. Bioelectron.*, 105 (2018) 14-21.
12. M.M. Musameh, C.J. Dunn, M.H. Uddin, T.D. Sutherland, T.D. Rapson, *Biosens. Bioelectron.*, 103 (2018) 26-31.
13. A. Kaushik, S. Tiwari, R.D. Jayant, A. Vashist, R. Nikkhah-Moshaie, N. El-Hage, M. Nair, *Trends Biotechnol.*, 35(4) (2017) 308-317.
14. S. Tanaka, Y.V. Kaneti, R. Bhattacharjee, M.N. Islam, R. Nakahata, N. Abdullah, S.I. Yusa, N.T. Nguyen, M.J.A. Shiddiky, M.S.A. Hossain, Y. Yamauchi, *ACS Appl. Mater. Interfaces*, 10(1) (2018) 1039.
15. M. Sajid, M.K. Nazal, M. Mansha, A. Alsharaa, S.M.S. Jillani, C. Basheer, *TrAC, Trends Anal. Chem.*, 76 (2016) 15-29.
16. F. Pepi, A. Tata, S. Garzoli, P. Giacomello, R. Ragno, A. Patsilnakos, M.D. Fusco, A. D'Annibale, S. Cannistraro, C. Baldacchini, G. Favero, M. Frasconi, F. Mazzei, *J. Phys. Chem. C*, 115(11) (2011) 4863-4871.
17. G. Pankratova, K. Hasan, D. Leech, L. Hederstedt, L. Gorton, *Electrochem. Commun.*, 75 (2017) 56-59.
18. M.-T. Hsieh, T.-J. Whang, *Appl. Surf. Sci.*, 396 (2017) 1589-1595.
19. W. Sun, J. Han, K. Jiao, L. Lu, *Bioelectrochemistry*, 68(1) (2006) 60-66.
20. R. Zhang, G.-D. Jin, D. Chen, X.-Y. Hu, *Sens. Actuators, B*, 138(1) (2009) 174-181.
21. S. Yang, G. Li, J. Zhao, H. Zhu, L. Qu, *J. Electroanalytical Chem.*, 717-718 (2014) 225-230.
22. N. He, R.E. Gyurcsanyi, T. Lindfors, *Analyst.*, 141(10) (2016) 2990-7.
23. P.V. Narayana, T.M. Reddy, P. Gopal, G.R. Naidu, *Anal. Methods*, 6(23) (2014) 9459-9468.
24. E.B. Bahadır, M.K. Sezgingtürk, *TrAC, Trends Anal. Chem.*, 76 (2016) 1-14.
25. C. Gardin, A. Piattelli, B. Zavan, *Trends Biotechnol.*, 34(6) (2016) 435-437.
26. N. Dubey, K. Ellepola, F.E.D. Decroix, J.L.P. Morin, A.H. Castro Neto, C.J. Seneviratne, V. Rosa, *Nanotoxicology*, 12(4) (2018) 274-289.
27. X. Lin, Y. Ni, S. Kokot, *J. Hazard. Mater.*, 260 (2013) 508-17.
28. F. Furno, K.S. Morley, B. Wong, B.L. Sharp, P.L. Arnold, S.M. Howdle, R. Bayston, P.D. Brown, P.D. Winship, H.J. Reid, *J. Antimicrob. Chemother.*, 54(6) (2004) 1019-1024.
29. V. Marassi, L.D. Cristo, S.G.J. Smith, S. Orтели, M. Blosi, A.L. Costa, P. Reschiglian, Y. Volkov, A. Prinamello, *Royal Society Open Science*, 5(1) (2018) 171113.
30. X. Liu, X. Liu, H. Wei, G. Song, H. Guo, X. Lu, *Sens. Actuators, B*, 252 (2017) 503-510.
31. F. Li, X. Jiang, J. Zhao, S. Zhang, *Nano Energy*, 16 (2015) 488-515.
32. Y. Song, J. Yang, K. Wang, S. Haller, Y. Wang, C. Wang, Y. Xia, *Carbon*, 96 (2016) 955-964.
33. K. Fuchs, *Proc. Camb. Phil. Soc.* 11 (1938), 100-108.
34. T. Zhana, Z. Tana, X. Wanga, W. Houb, *Sens. Actuators, B*, 255 (2018) 149-158.
35. L. Shen, N. Hu, *Biochimica et Biophysica Acta* 1608 (2004) 23-33.
36. Y. Liu, M. Wang, F. Zhao, Z. Guo, H. Chen, S. Dong, *J. Electroanal. Chem.*, 581 (2005) 1-10.
37. E. Laviron, *J. Electroanal. Chem.*, 101(1) (1979) 19-28.

38. D. Jia, L. Wang, Y. Gao, L. Zou, B. Ye, *J. Electroanal. Chem.*, 764 (2016) 56-63.
39. F. Manea, M. Ihos, A. Remes, G. Burtica, J. Schoonman, *Electroanalysis*, 22(17-18) (2010) 2058-2063.
40. M. Shalauddin, S. Akhter, S. Bagheri, M.S. Abd Karim, N. Adib Kadri, W.J. Basirun, *Int. J. Hydrogen Energy*, 42(31) (2017) 19951-19960.
41. L. Kashefi-Kheyrabadi, M.A. Mehrgardi, *Biosens. Bioelectron.*, 33(1) (2012) 184-9.
42. G.P. Fard, E. Alipour, R.E. Ali Sabzi, *Anal. Methods*, 8(19) (2016) 3966-3974.
43. A. Mokhtari, H. Karimi-Maleh, A.A. Ensafi, H. Beitollahi, *Sensors and Actuators B: Chemical*, 169 (2012) 96-105.
44. B.K. Chethana, S. Basavanna, Y. Arthoba Naik, *Ind. Eng. Chem. Res.*, 51(31) (2012) 10287-10295.
45. M. Arvand, T. M. Gholizadeh, M. A. Zanjanchi, *Materials Science and Engineering C*, 32 (2012) 1682–1689.
46. A. A. Ensafi & M. Izadi & H. Karimi-Maleh, *Ionics*, (2013) 19:137–144.
47. C. Karuppiah, S. Cheemalapati, S.M. Chen, S. Palanisamy, *Ionics*, 21 (2014) 231.
48. Y. XF, W. SH, *Mater Sci Eng C*, (2010) 28:188.
49. A. Ambrosi, R. Antiochia, L. Campanella, R. Dragone, I. Lavagnini, *J Hazard Mater*, (2005) 122:219.

© 2019 The Authors. Published by ESG ([www.electrochemsci.org](http://www.electrochemsci.org)). This article is an open access article distributed under the terms and conditions of the Creative Commons Attribution license (<http://creativecommons.org/licenses/by/4.0/>).